ELSEVIER

Biophysical Chemistry 125 (2007) 508 – 520

Biophysical Chemistry

http://www.elsevier.com/locate/biophyschem

RNA binding small molecules: Studies on t-RNA binding by cytotoxic plant alkaloids berberine, palmatine and the comparison to ethidium

Md. Maidul Islam, Rangana Sinha, Gopinatha Suresh Kumar *

Biophysical Chemistry Laboratory, Indian Institute of Chemical Biology, 4, Raja S. C. Mullick Road, Kolkata 700032, India

Received 6 June 2006; received in revised form 3 November 2006; accepted 3 November 2006
Available online 10 November 2006

Abstract

The interaction of two natural protoberberine plant alkaloids berberine and palmatine with t-RNA^{phe} was studied using various biophysical techniques and the data was compared with the binding of the classical DNA intercalator, ethidium. The results of optical thermal melting, differential scanning calorimetry and circular dichroism characterized the native cloverleaf structure of t-RNA under the conditions of the study. The strong binding of the alkaloids and ethidium to t-RNA was revealed from the absorption and fluorescence studies. The salt dependence of the binding constants enabled the dissection of the binding free energy to electrostatic and non-electrostatic contributions. This analysis revealed a surprisingly large favourable component of the non-electrostatic contribution to the binding of these charged alkaloids and ethidium to t-RNA. Isothermal titration calorimetric studies revealed that the binding of both the alkaloids is driven by a moderately favourable enthalpy decrease and a moderately favourable entropy increase while that of ethidium is driven by a large favourable enthalpy decrease. Taken together, the results suggest that the binding of these alkaloid molecules on the t-RNA structure appears to be mostly by partial intercalation while ethidium intercalates to the t-RNA. These results reveal the molecular aspects on the interaction of these alkaloids to t-RNA.

Keywords: Protoberberine alkaloids; t-RNA; Alkaloid-t-RNA interaction; Spectroscopy; Calorimetry; Thermodynamics

1. Introduction

Interaction between small molecules and nucleic acids has been an active area that has received considerable attention in the past several years [1–4]. The impetus for these studies has been the desire to understand the molecular basis of drug action. Extensive studies have led to the discovery of a large number of lead compounds that range from natural products to purely synthetic designs that can bind in a variety of surprising ways to DNA modulating various biological activities. These molecules serve as lead compounds in studies of protein–nucleic acid recognition, provide site specific reagents for molecular biology and serve as potential guides for the rational design of new therapeutic agents. Intercalation and groove binding represent two major noncovalent binding modes of small molecules to DNA and knowledge on the molecular aspects of these binding modes have significantly advanced the development of more efficacious anticancer agents. In contrast to DNA, over a period of time very little attention has been paid to the recognition of RNA by small molecules. This has been partly due to the complex structural diversity of the RNAs in comparison to DNA and the relatively scanty high-resolution structural information available in respect of RNA molecules. Nevertheless, since the knowledge that many serious diseases are caused by RNA viruses and particularity after the emergence of RNA viruses like HIV and Hepatitis C, there has been growing interest in the development of RNA binding antiviral compounds and RNA based anticancer agents [5–9]. A rational design of such RNA based therapeutics molecules however would essentially require a detailed knowledge of the structural aspects of RNA on one hand and the molecular nature of the mode, mechanism and specificity of binding of small molecules to various conformations of RNA on the other hand. In the past several years significant advancement has taken place in the structural evaluation of various RNAs [10,11]. Although all cellular RNAs have single polynucleotide chain, they are highly versatile molecules that can fold into a multitude of secondary

* Corresponding author. Tel.: +91 33 2472 4049; fax: +91 33 2473 0284/5197.
E-mail address: gskumar@iicb.res.in (G.S. Kumar).

0301-4622/$ - see front matter © 2006 Elsevier B.V. All rights reserved.
doi:10.1016/j.bpc.2006.11.001

structures and conformations. These complex structural motifs could be potential binding pockets for specific drug recognition sites and it would be interesting to take advantage of these promising recognition capabilities of RNAs to develop new RNA binders as modulators of cellular functions [12–14]. Studies in this direction have identified different class of RNA binding compounds, of which the most important are the aminoglycoside antibiotics that was shown to interact with the functional sites on 16S rRNA [15,16]. One approach to the development of RNA targeted drug has been to study the interaction of known DNA binding compounds with fairly well characterized interaction profiles. Wilson and coworkers have initiated work in this direction and have performed interaction of a wide variety of DNA intercalating and groove binding molecules with various RNA constructs [5,17–19]. As part of antigene strategy, studies with many RNA triplexes were also performed [20,21]. Our primary interest has been to enhance the fundamental knowledge in this area by studying the binding of some natural alkaloids with t-RNA structures. t-RNAs are versatile molecules with cloverleaf structure that show high degree of folding stabilized by base stacking, base pairing and other tertiary interactions. t-RNA^{phe} (Fig. 1) is one of the most thoroughly characterized naturally occurring RNA molecule available for such interaction study. Natural products in general due to their unmatched chemical diversity and biological relevance have been widely accepted as potential high quality pools in drug screening. In this context, our previous studies have identified the protoberberine alkaloids berberine and palmatine to be lead compounds that exercise high specificity to single stranded poly(A) molecules [22–25]. A subsequent study by Xing et al. [26] on the closely related synthetic molecule coralyne further confirmed the high specificity of protoberberine related compounds to poly(A). Protoberberines are now extensively studied and being known to be important lead compounds in cancer therapy of which berberine and palmatine

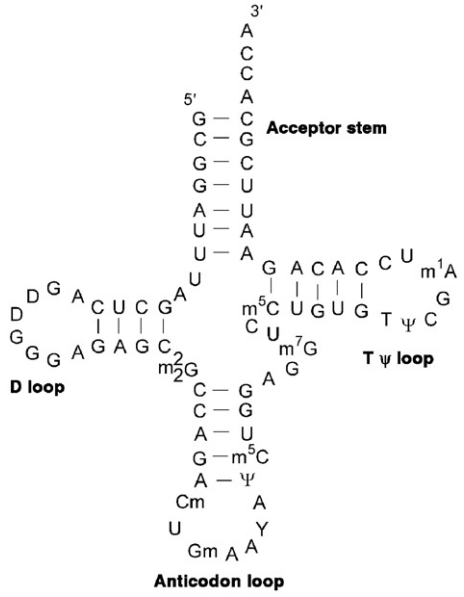

Fig. 1. The cloverleaf structure of yeast t-RNA^{phe}.

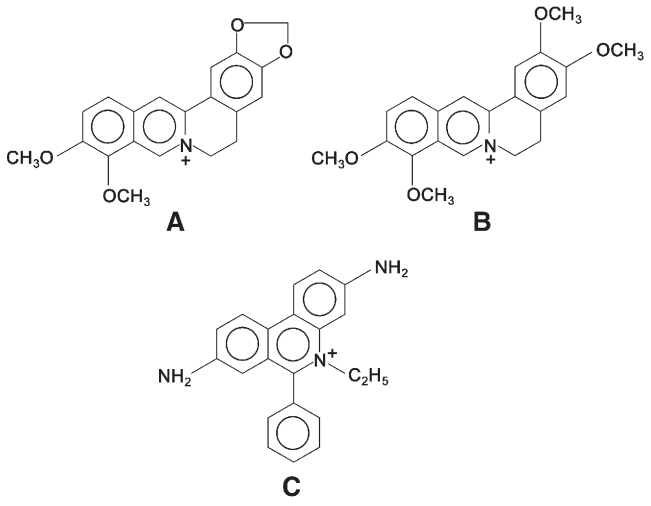

Fig. 2. Chemical structure of (A) berberine, (B) palmatine and (C) ethidium.

(Fig. 2A and B) are the two most prominent members. Plants containing these alkaloids have been used as folk medicines for centuries world over without a clear understanding of their molecular bio-targets. Berberine and palmatine have wide range of biochemical and pharmacological effects [27–29] and were demonstrated to possess antitumor activity in vitro and in vivo [30–33]. Berberine induces apoptosis through a mitochondria/caspase pathway in human hepatoma cells [34]. Both the alkaloids have been known to bind to DNA predominantly by intercalation exhibiting remarkable adenine–thymine base pair specificity [35–40]. In view of their remarkably strong binding to poly(A) we sought to study the interaction of these two natural alkaloids with other RNA structures with the long-range goal of developing RNA based therapeutic agents. In this paper we present the results of our investigation on the binding of berberine and palmatine to t-RNA and compare it with the t-RNA–ethidium (Fig. 2C) complexation from multifaceted spectroscopic, thermal melting, viscometric, ultra sensitive titration and differential scanning calorimetric studies.

2. Experimental

2.1. RNA and drugs

t-RNA^{Phe} (yeast) was purchased from Sigma-Aldrich Corporation (St. Louis, MO, USA). Its concentration was determined spectrophotometrically using a molar extinction coefficient (ε) 6900 (M^{-1} cm^{-1}) at 258 nm expressed in terms of nucleotide phosphates [41]. The ratio of the absorbance at 260 to 280 nm indicated that the sample was free from protein contaminations. Berberine chloride, palmatine chloride and ethidium bromide were obtained from Sigma-Aldrich and were used without further purification as no detectable impurities were observed by thin layer chromatography and ^{1}H NMR spectroscopy. Drug solutions were freshly prepared each day and were always kept protected in the dark to prevent any light induced photochemical changes. Molar extinction coefficients (ε) of 22,500 M^{-1} cm^{-1} (at 344 nm) for berberine, 25,000 M^{-1} cm^{-1} (at 345 nm) for palmatine and

5680 M^{-1} cm^{-1} (at 480 nm) for ethidium were used for determining their concentrations by absorbance measurements. No deviation from Beer's law was observed in the concentration range employed in this study.

All experiments were conducted in Citrate-Phosphate (CP) buffer (1 mM [Na^+]), pH 7.0, containing 0.5 mM Na_2HPO_4. pH was adjusted using citric acid [42,43]. Glass distilled deionized water and analytical grade reagents were used throughout. pH measurements were made on an Electronic Corporation (India) pH meter with an accuracy of ±0.01 units. All buffer solutions were filtered through Millipore filters of 0.45 μm before use.

2.2. Circular dichroism

Circular dichroism (CD) measurements were carried out on a PC controlled JASCO J715 spectropolarimeter (Japan Spectroscopic Ltd., Japan) equipped with a JASCO temperature controller (model PTC 343) at 25±0.5 °C as reported earlier [9,44]. A rectangular quartz cell of 1 cm path length was used for CD measurements. Each spectrum was averaged from five successive accumulations at a scan rate of 100 nm min^{-1} keeping a bandwidth of 1.0 nm at a sensitivity of 100 milli degree and was base line corrected and smoothed within permissible limits using the inbuilt software of the unit. The molar ellipticity values [θ] are expressed in terms of either per nucleotide (210–400 nm) or per bound ligand (300–500 nm in case of alkaloids and 300–700 in case of ethidium). Temperature dependent spectra in the range 5–15 °C were acquired with continuous purging of dry nitrogen gas in the sample chamber to prevent condensing of moisture on the optical windows. The spectropolarimeter was routinely calibrated using an aqueous solution (w/v) of d-10 ammonium camphor sulphonate.

2.3. Absorbance titration

The absorption spectra of the drugs mixed with or without RNA were obtained at 25±0.5 °C using a Shimadzu PharmaSpec 1700 spectrophotometer (Shimadzu Corporation, Japan) in matched quartz cells of 1 cm path length. Titrations were performed keeping a constant concentration of the ligand and varying the t-RNA concentration following generally the methods described earlier [45].

2.4. Fluorescence titration

Steady state fluorescence measurements were performed on a Hitachi F4010 fluorescence spectrometer (Hitachi Ltd., Tokyo, Japan) in fluorescence free quartz cells of 1 cm path length as described previously [9] where a fixed concentration of the ligand was titrated with increasing concentrations of t-RNA. The excitation wavelength for berberine and palmatine was 350 nm while the same for ethidium was 510 nm. All measurements were done keeping excitation and emission band passes of 5 nm. The sample temperature was maintained at 25±0.5 °C using Eylea Uni Cool U55 water bath (Tokyo Rikakikai, Japan). Uncorrected fluorescence spectra are reported.

2.5. Evaluation of binding stoichiometry of ligand–t-RNA complexation

JOBS continuous variation method [46,47] was applied to determine the binding stoichiometries. At constant temperature (25 °C), the fluorescence signal was recorded for solutions where the concentration of both t-RNA and ligand were varied while the sum of their concentrations was kept constant at 80 μM. ΔF_{530} in case of the alkaloids and ΔF_{605} in the case of ethidium (the difference in the fluorescence intensity of the ligand in the absence and presence of t-RNA) was plotted as a function of the input mole fraction of the ligand (χ). Break point in the resulting plot corresponds to the mole fraction of the ligand in the complex. The stoichiometry is obtained in terms of t-RNA–ligand [$(1-\chi_{ligand})$: χ_{ligand}], where χ_{ligand} denotes mole fraction of ligands.

2.6. Determination of affinity constants

Binding affinities of the compounds to t-RNA were evaluated from absorbance and fluorescence titrations. From the titration data the concentrations of bound (C_b) and the free ligand (C_f) were determined from the absorbance or fluorescence change at a fixed wavelength, which usually corresponds to the wavelength of maximum change (344 and 345 nm in case of berberine and palmatine and 480 nm in the case of ethidium). If $A_F(I_F)$, $A_B(I_B)$, and $A(I)$ represent respectively, the absorbance (or fluorescence) of the initially, finally, and partially titrated ligands, then the fraction of the bound ligand molecules (α_b) would be given by

$$\alpha_b = A_F(I_F) - A(I) / A_F(I_F) - A_B(I_B). \quad (1)$$

The molar concentration of free and bound ligand molecules and r, the number of moles of ligand bound per mole of nucleotide could be evaluated from the following equations where D and P represent the total input ligand and RNA nucleotide phosphate concentration respectively

$$C_f = (1-\alpha_b)D \quad (2)$$

$$C_b = \alpha_b D \quad (3)$$

$$r = C_b/P = \alpha_b D/P. \quad (4)$$

Binding data obtained from spectrophotometric and spectrofluorimetric titrations were cast into Scatchard plot of r/C_f versus r. Non-linear binding isotherms obtained in each case were fitted to a theoretical curve drawn according to the excluded site model [48] developed by McGhee and von Hippel for a non-linear non-cooperative ligand binding system using the following equation

$$\frac{r}{C_f} = K_i(1-nr)\left[\frac{(1-nr)}{\{1-(n-1)r\}}\right]^{(n-1)} \quad (5)$$

where K_i is the intrinsic binding constant to an isolated binding site, and n is the number of nucleotides excluded by the binding of a single ligand molecule. The binding data were analyzed using the software programme Scatplot [49] version 1.2 that works on an algorithm that determines the best-fit parameters to (5) as described earlier [44,45].

2.7. Solution viscosity measurements

Viscometry studies used a Cannon-Manning semi micro dilution viscometer type 75 (Cannon Instruments Co., State College, PA, USA) submerged vertically in a constant temperature water bath (Cannon Instruments Co.) maintained at 25±0.5 °C. 600 μL of t-RNA solution (700 μM) was placed in the viscometer and aliquots of stock solution of the compounds under study were directly added into the viscometer to obtain increasing D/P [drug (ligand)/nucleotide phosphate molar ratio] values. Bubbling dry nitrogen gas slowly through the viscometer ensured mixing of the solution. Flow times of sample alone and sample with different ratio of the ligands were measured in triplicate with an accuracy of ±0.01 s using a Casio model HS-30W electronic stop watch (Casio Computer Co. Ltd, Japan) and the relative specific relative viscosity was calculated using the equation

$$\eta'_{sp}/\eta_{sp} = [(t_{complex}-t_o)/t_o]/[t_{control}-t_o/t_o] \quad (6)$$

where η'_{sp} and η_{sp} are the specific viscosity of t-RNA in the presence and absence of the ligands and $t_{complex}$, $t_{control}$ are the average efflux times of complex and RNA and t_o is the same for the buffer as described previously [9,50].

2.8. Isothermal titration calorimetry

Isothermal titration calorimetric (ITC) experiments were performed at 25 °C (298 K) on a MicroCal VP-ITC unit (MicroCal, Inc.; Northampton, MA, USA). The t-RNA solution was dialyzed against the buffer and the dialysate was used for the preparation of the ligand solutions. Prior to use all the solutions were thoroughly degassed by stirring under vacuum (140 mbar, 8 min) on the Microcal's Thermovac unit to eliminate air bubbles. The ITC cell was filled with the ligand solution (20 μM berberine or ethidium and 25 μM palmatine) and was titrated with the RNA solution (2.8 mM in case of titration to berberine or palmatine and 1 mM for titration to ethidium) from the syringe. Origin 7.0 software, supplied by Microcal was used for data acquisition and manipulation. In a typical experiment each titration consisted of several injections. Corresponding control experiments to determine the heat of dilution were performed by injecting the t-RNA in the same protocol to the buffer alone. The heat signal of this control was then subtracted from the raw data for each titration. The area under each peak was determined by integration using the Origin software to give the measure of the heat associated with the injection. The heat associated with each RNA-buffer was subtracted from the corresponding heat associated with each RNA-alkaloid injection to give the heat of alkaloid binding for that injection. The heat of dilution of injecting the ligands into the buffer alone was observed to be negligible. The resulting data were analyzed using Origin software to estimate the binding affinity (K_b), the binding stoichiometry (N) and the enthalpy of binding (ΔH^o). The free energies (ΔG^o) were calculated using the standard relationship

$$\Delta G^o = -RT\ \ln(K_b). \quad (7)$$

The binding free energy coupled with the binding enthalpies derived from the ITC data allowed the calculation of the entropic contribution to the binding ($T\Delta S^o$), where $T\Delta S^o$ is the calculated binding entropy using the standard relationship

$$T\Delta S^o = \Delta H^o - \Delta G^o. \quad (8)$$

2.9. Differential scanning calorimetry

To investigate the helix-coil transition of t-RNA, excess heat capacities as a function of temperature were measured on a Microcal VP-differential scanning calorimeter (DSC) (MicroCal, Inc.; Northampton, MA, USA). The t-RNA sample for DSC measurement was prepared exactly like that for ITC. The instrument base line was determined before the sample scans by filling both reference and sample cells with the same dialysate buffer. The sample cell of the calorimeter containing 0.52 mL of the t-RNA solution (2 mM) and the reference cell containing the same volume of the buffer solution were heated from 10 to 100 °C employing the same scanning parameters used for the base line scanning. Typically a scan rate of 60 °C/h was set for the heating cycle and each experiment involved at least three separate filling of the DSC cell. Each experiment was repeated twice with separate fillings. After buffer subtraction and base line adjustments, the DSC thermograms depicting excess heat capacity versus temperature plots were analyzed using the Origin 7.0 software. The thermograms were deconvoluted considering three transitions and were carried out using the Non-2-State with zero DCp model of Origin fitting. The analysis gave values for the melting temperatures, T_m and the calorimetric and van't Hoff enthalpies for the transitions. To check the reversibility of the transition, the sample was allowed to cool slowly to 10 °C (10 °C/h) and a repeat DSC scan was performed on the renatured sample under identical conditions.

2.10. UV optical melting study

Absorbance versus temperature profiles (melting curves) of t-RNA were measured on the Shimadzu Pharmaspec 1700 unit equipped with the peltier controlled TMSPC-8 model accessory (Shimadzu Corporation, Japan). In a typical experiment, the RNA sample was mixed and diluted into the desired degassed buffer in the micro optical cuvettes of 1 cm path length and the temperature of the microcell accessory was raised at a heating rate of 0.5 °C/min while continuously monitoring the absorbance change at 260 nm. Melting curves allowed an

estimation of melting temperature, T_m, the midpoint temperature of the unfolding process. The, van't Hoff enthalpy, ΔH_{VH} was calculated using the equation [51]

$$\Delta H_{vh} = (2+2n)RT_m^2(\delta\alpha/\delta T)_{T=T_m} \quad (9)$$

where α is the fraction of single strands in the duplex state.

3. Results

3.1. pH and temperature dependent conformation of t-RNA from circular dichroism

The effect of varying the pH in the range 7.0 to 3.1 and temperature from 5 to 90 °C on the t-RNA conformation was studied using circular dichroism spectroscopy. The effect of pH on the CD spectrum of t-RNA is depicted in Fig. 3A. The t-RNA CD spectrum at the physiological pH showed typical A-form RNA conformation having a large positive band around 269 nm and a small trough around 235 nm and is in agreement to that reported by other workers [22,41]. On lowering the pH, there were significant perturbations in the CD spectrum, being manifested by small bathochromic shifts and large hypochromic effects in the 269 nm band. At pH 3.1, the CD spectrum of the t-RNA has a CD maximum around 272 nm but with almost one third of the ellipticity at neutral pH. On raising the pH, the ellipticity regained and it was observed that at pH 7.0 the t-RNA CD spectrum was almost superimposed with the native spectrum indicating more or less a complete reversal of the pH dependent conformational changes. A plot of the change in the ellipticity of the 269 nm band versus pH is depicted in the inset of Fig. 3A.

The effect of temperature on the CD spectrum of t-RNA is presented in Fig. 3B. Almost similar change like that observed on pH variation was observed here also up to a temperature of 90 °C indicating disruption of ordered structure of t-RNA. On renaturation, the RNA almost attained the original structure as reveled by the complete reversal of the CD spectrum. The variation of the ellipticity of the 269 nm band with temperature is given in the inset of Fig. 3B.

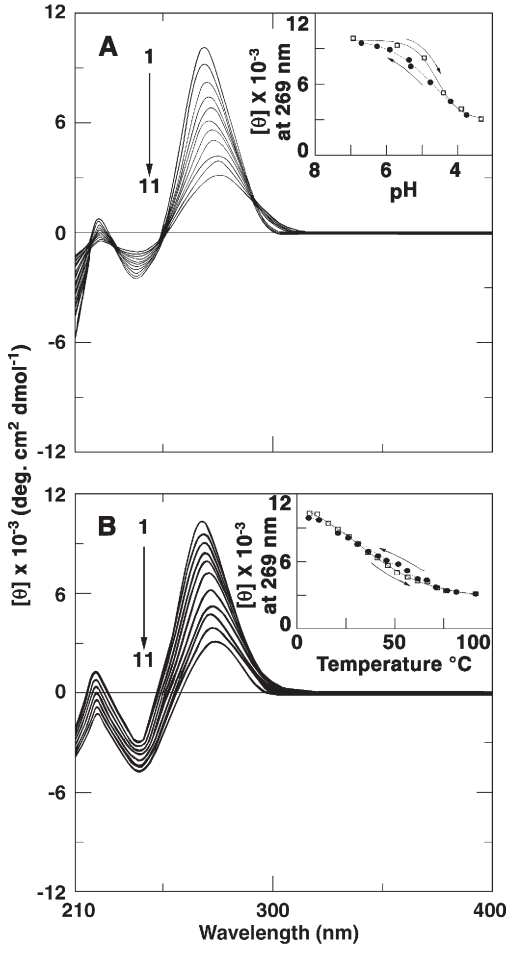

Fig. 3. (A) pH and (B) temperature dependent change of CD spectrum of t-RNA. Curves (1–11) in (A) denote pH values of 7.00, 6.41, 5.50, 5.16, 4.85, 4.78, 4.60, 4.30, 3.97, 3.59, and 3.10 and in (B) denote temperature of 5, 13, 17.8, 22.8, 28.4, 34.9, 46.2, 56.7, 63.2, 75.15, and 89.8 °C respectively in CP buffer. Inset: Variation of molar ellipticity [θ] of the 269 nm band with pH and temperature. The arrows indicate the direction of pH and temperature change.

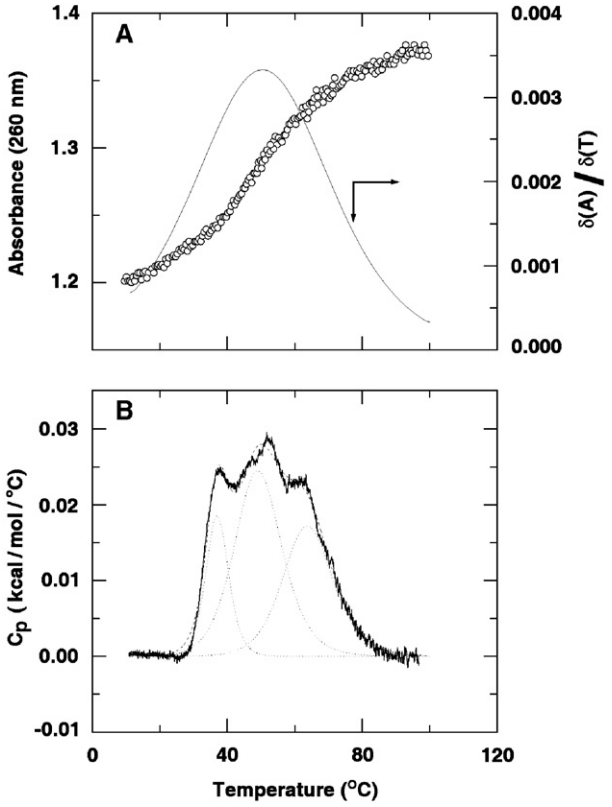

Fig. 4. (A) Representative optical thermal melting profile of t-RNA (174 μM) and (B) DSC thermogram of t-RNA (2 mM) in CP buffer of pH 7.0. The continuous line in the top panel represents the differential curve to the melting profile. Deconvolution of the recorded DSC thermogram (bottom panel) was carried out fitting using a function of three Gauss curves (dotted lines) The cumulative Gauss curve (dashed line) describes the experimental curve satisfactorily.

Table 1
Apparent thermal transition temperatures (T_m) and estimated heat values of the individual calorimetric transitions of denaturation of t-RNA[a]

Parameters	Transition 1	Transition 2	Transition 3
T_m (°C)	37.0±0.2	49.3±0.2	64.0±0.3
ΔH^b_{cal} (cal/mol)	166.4±4.2	457.7±11.7	339.2±8.2
ΔH^c_v (kcal/mol)	85.1±1.1	44.1±0.8	45.7±0.5

[a]Average of two determinations in CP buffer containing 0.5 mM Na_2HPO_4, pH 7.0. [b]Calorimetric enthalpy. [c]van't Hoff enthalpy.

3.2. UV thermal melting

Fig. 4A shows the optical thermal melting profile of the t-RNA in the temperature range 10–100 °C. It can be seen that the melting curve exhibited a broad but cooperative transition spanning over a temperature of about 50 °C with a hyperchromicity change of about 15%. From the differential plot an average T_m value of 48±1 °C was observed. Using this T_m value, a van't Hoff enthalpy of 19.8 kcal/mole was calculated for the unfolding of the t-RNA. The melting studies of t-RNA at different [Na^+] ion concentrations between 1 and 50 mM (not shown) revealed that the average melting temperatures increased as the [Na^+] increased without any significant change in the overall nature of the transition or hyperchromicty and at 50 mM [Na^+] the T_m of the RNA was 56±1 °C. It follows from the optical thermal melting experiments that the t-RNA structure retains the native cloverleaf structure that underwent heat denaturation and it appears that no prior disruption of the structure had occurred under the conditions of our study. The melting curve was almost superimposable when the sample was slowly cooled to 10 °C and a second thermal denaturation experiment was performed on the sample (not shown).

3.3. Differential scanning calorimetry

Differential scanning calorimetric (DSC) melting of the t-RNA sample in the temperature range 10–100 °C was studied to further understand the nature of the thermal unfolding and complexity, if any, in the denaturation pattern under the condition of our experiments. The DSC thermogram (Fig. 4B) represents a broad and asymmetric endothermic transition with a maximum at ~50 °C with two shoulders. The maxima of the three deconvoluted DSC bands when considering three transitions were at 37.0±0.2 °C, 49.3±0.7 °C and 64.0±0.3 °C respectively. We have observed that increasing [Na^+] concentration from 1 to 50 mM gave similar results with three transitions, but the T_m values of the second and third transitions shifted to higher temperatures. For the first transition no shift was observed (T_m=37.0±0.2 °C). On the contrary, a large shift for the second transition (T_m from 49.3±0.7 °C to 60.5±0.3 °C) and third transition (T_m from 64.0±0.3 °C to 76.6±0.4 °C) were observed (not shown). The thermal melting temperatures and the associated van't Hoff and calorimetric enthalpy of these individual transitions are depicted in Table 1.

3.4. Binding stoichiometry

The binding stoichiometry and the possible number of binding sites of berberine, palmatine and ethidium to t-RNA were determined by continuous variation analysis (Job plots) in fluorescence (Fig. 5A–C). The plots of difference fluorescence intensity at 530 nm for berberine and palmatine and at 605 nm for ethidium versus the mole fraction of the ligand revealed a single binding mode for the binding of the alkaloids and ethidium on t-RNA. From the inflection points at χ_{ligand}=0.11, 0.09 and 0.18 for berberine, palmatine and ethidium, the number of nucleotides per one ligand can be estimated as 8.1, 10.1 and 4.6 respectively.

3.5. Spectrophotometric studies

Binding of berberine, palmatine to t-RNA was studied by more rigorous spectrophotometric titration and was compared

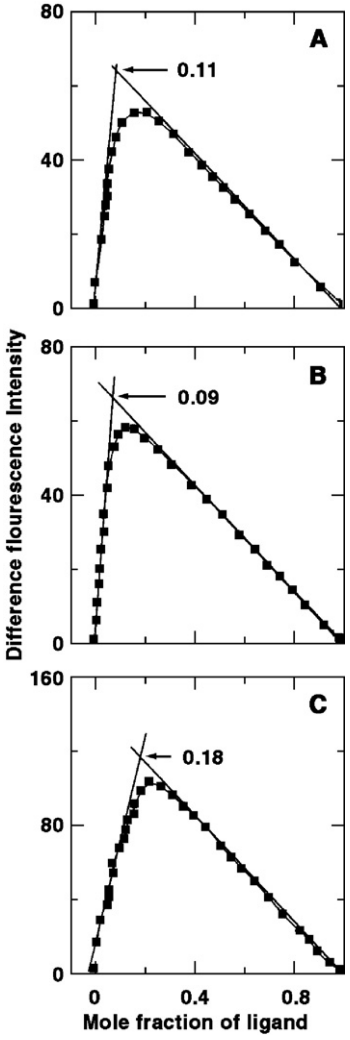

Fig. 5. Jobs plot for (A) berberine (B) palmatine and (C) ethidium binding to t-RNA in CP buffer of pH 7.0 at 25 °C. The different fluorescence intensity at 530 nm for berberine and palmatine and at 605 nm for ethidium was plotted against the mole fraction of the drug added.

with the binding of ethidium under identical condition. In Fig. 6, the spectrophotometric titrations of a fixed concentration of these compounds with increasing concentration of t-RNA are

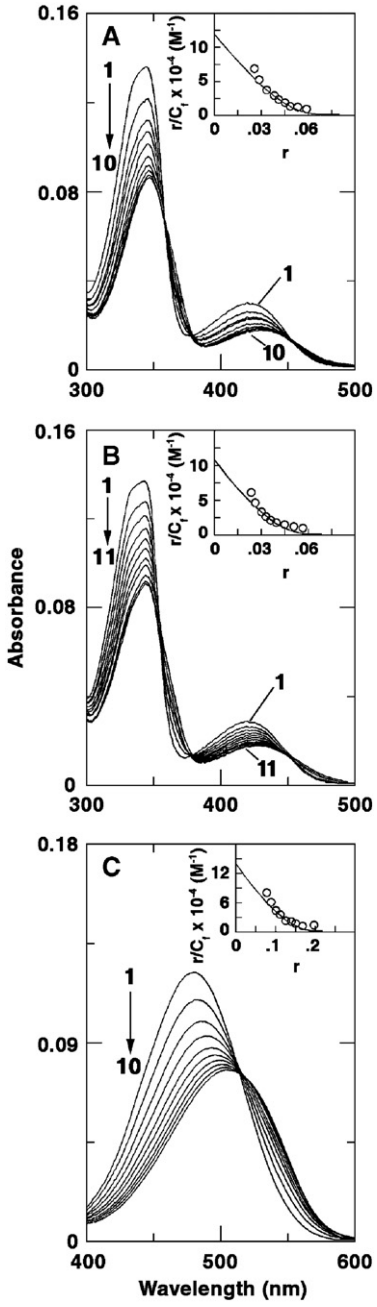

Fig. 6. Representative absorbance spectra of (A) berberine (6.04 μM) treated with 0, 26.60, 53.20, 79.80, 106.40, 133.00, 159.60, 186.20, 212.80, and 239.40 μM (curves 1–10) (B) palmatine (5.44 μM) treated with 0, 21.89, 43.78, 65.67, 87.56, 109.45, 131.34, 153.23, 175.12, 197.01, and 218.90 μM (curves 1–11) and (C) ethidium (21.47 μM) treated with 0, 26.35, 52.70, 79.06, 105.41, 131.76, 158.12, 184.47, 210.82, and 237.18 μM (curves 1–10) of t-RNA. All experiments were performed at 25 °C in CP buffer of pH 7.0. Inset: representative Scatchard plot of each complexation. The solid lines represent the non-linear least square best-fit of the experimental points to the neighbor exclusion model [48] obtained using the software Scatplot [49]. The best-fit data are in the range of 30–35% (lower limit) and 85–90% (upper limit). Values of K_i (intrinsic binding constant) and n (number of excluded sites) are presented in Table 2.

Table 2
Summary of the optical properties of free and bound ligands[a]

	Berberine	Palmatine	Ethidium
Absorbance			
λ_{max} (free)	344	345	480
λ_{max} (bound)	348	348	505
λ^{b}_{iso}	360, 379, 454	360, 379, 454	515
ε_f (at λ_{max})	22,500 (344)	25,000 (345)	5680
ε_b (at λ_{max})	14,030 (348)	16,317 (346)	3635
Fluorescence			
λ_{max} (ex)	350	350	510
λ_{max} (em)	530	530	605
F_b/F_o	42.64	29.78	15.13

[a]Units: λ nm; ε (molar extinction coefficient) M^{-1} cm^{-1}; [b]Wavelengths at the isosbestic point.

presented. Binding to t-RNA resulted in significant changes in the absorption spectra of these compounds. Hypochromic and bathochromic effects with sharp isosbestic points were obtained in all the cases indicating an effective overlap of the π electron cloud of the alkaloids and ethidium with the base pairs of t-RNA. While with the alkaloids (Fig. 6A and B) three isosbestic points were observed at 360, 379 and 454 nm respectively, the ethidium titration (Fig. 6C) was characterized by one single isosbestic point at 515 nm. The optical properties of berberine, palmatine and ethidium, and that of their complexes with t-RNA are depicted in Table 2.

3.6. Spectrofluorimetric studies

Berberine and palmatine are weak fluorescent compounds while ethidium is a strong fluorophore. Both the alkaloids have fluorescence emission spectra in the 450–550 nm range when excited at 350 nm while ethidium has a fluorescence maximum at 605 nm when excited at 510 nm. Binding to DNA is known to remarkably enhance the fluorescence of all these compounds [35]. Binding to t-RNA also resulted in increase of the fluorescence of all the three compounds (not shown) eventually leading to saturation. The enhancement of fluorescence intensity on complexation was similar in the alkaloids, but more pronounced in the case of ethidium. Large fluorescence enhancement in each case is indicative of strong association of these molecules to t-RNA structure and also proposing the location of the bound molecules in hydrophobic environment.

3.7. Binding parameters

The result of spectrophotometric and spectrofluorimetric titrations were expressed in the form of Scatchard plots of r/C_f versus r. The binding constants and the number of excluded sites for the interaction of these compounds to t-RNA were estimated from Scatchard plots. The binding isotherm in each case was non-linear and concave upwards, indicating a non-cooperative binding process. The Scatchard plots in each case derived from spectrophotometric studies and the non-linear least square fittings using the McGhee-von Hippel analyses are presented in the inset of Fig. 6. The quantitative binding parameters of berberine, palmatine and ethidium binding to t-RNA derived

Table 3
Binding parameters of t-RNA complexation with berberine, palmatine and ethidium obtained from spectrophotometric and spectrofluorimetric study[a]

Compound	Spectrophotometry		Spectrofluorimetry	
	$K_i/10^5$ (M^{-1})	n	$K_i/10^5$ (M^{-1})	n
Berberine	1.15±0.20	12.50±0.30	0.95±0.20	16.50±0.20
Palmatine	1.05±0.30	14.50±0.30	0.90 ± 0.15	17.50±0.25
Ethidium	1.38±0.30	4.60±0.20	1.20±0.27	7.40±0.30

[a]Average of four determinations. Binding constants (K_i) and the number of occluded sites (n) refer to solution conditions of CP buffer containing 0.5 mM Na_2HPO_4, pH 7.0 at 25 °C.

from these plots are collated in Table 3. The intrinsic binding affinity of berberine to t-RNA was $(1.15\pm0.20)\times10^5$ M^{-1} while that of palmatine has a value close at $(1.05\pm0.30)\times10^5$ M^{-1}. The binding affinity of ethidium to t-RNA estimated from similar analysis is marginally higher at $(1.38\pm0.30)\times10^5$ M^{-1}. Similarly, from spectrofluorimetric analysis values close to that obtained from spectrophotometry were obtained (Table 3). The similar values of binding constant for palmatine and berberine are indicative more or less similar affinity for these compounds to t-RNA. The numbers of excluded sites on binding of a single ligand molecule were found to be around 12, 14 and 5 and 16, 17 and 7 nucleotides respectively from spectrophotometric and spectrofluorimetric analysis for berberine, palmatine and ethidium.

3.8. Salt dependence of the binding

All the three compounds under investigation being positively charged, the effect of salt on the binding was studied by performing absorbance titration at five different salt conditions viz.1, 5, 10, 20 and 50 mM [Na^+] and the binding constants were evaluated under these salt concentrations. It was observed that the extent of hypochromic and bathochromic effects in the absorption spectra in each case showed some decrease as the ionic strength increased (not shown). In Fig. 7A, the variation of log K_i with log [Na^+] in each case is presented that revealed that the binding affinity falls by about 2.5 and 3.4 times respectively in berberine and palmatine while in case of ethidium the fall was lower and by about 1.7 times as the [Na^+] concentration increased from 1 to 50 mM. The slopes of these lines were found to be 0.24, 0.34 and 0.14 for berberine, palmatine and ethidium respectively. From the dependence of the binding constant (K_i) on salt concentration, the observed free energy (ΔG^o_{obsd}) can be partitioned into two contributions similar to that performed for many DNA binding ligands [52,53] namely, the non-polyelectrolytic contribution (ΔG_t) and the polyelectrolytic contribution (ΔG_{pe})

$$\Delta G^o_{obsd} = -RT\ln K = (\Delta G_t) + (\Delta G_{pe}). \quad (10)$$

The polyelectrolytic contribution at any given [Na^+] may be calculated from the experimentally determined quantity $((\delta\ln K/\delta\ln[Na^+]) = SK)$. Record and coworkers [54] have shown that $\Delta G_{pe} = -(SK)RT\ln[MX]$, where MX is the monovalent salt concentration. The magnitude of ΔG_{pe} is the

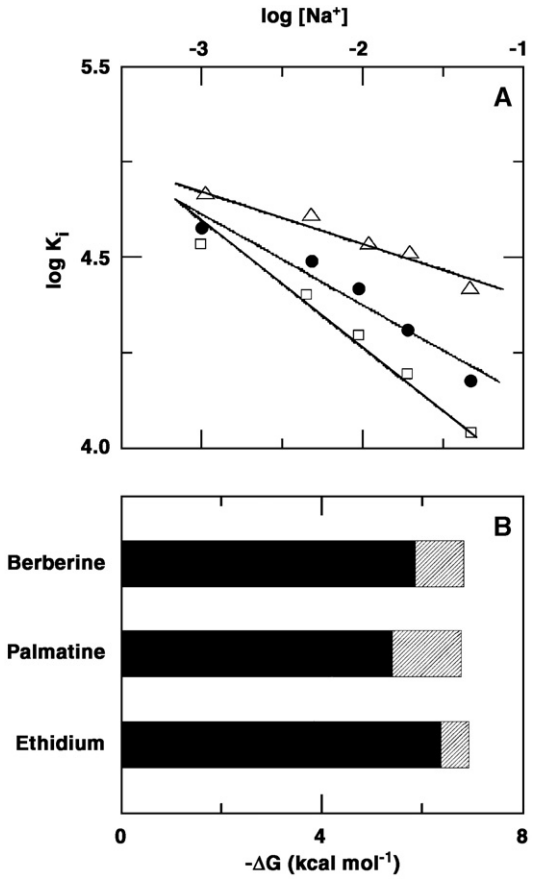

Fig. 7. (A) Log–log plot of intrinsic binding constant K_i as a function of ionic strength [Na^+] for berberine (●–●), palmatine (□–□) and ethidium (△–△) binding to t-RNA obtained from spectrophotometry in CP buffer pH 7.0 at 25 °C. The solid lines represent the best-fit to the experimental points (B) Polyelectrolyte (ΔG_{pe}) and non-electrostatic (ΔG_t) contribution to the binding free energy of berberine, palmatine and ethidium. The bar graph shows the contribution of ΔG_{pe} (hatched area) and ΔG_t (grey area) to the total binding free energy.

free energy contribution arising from coupled polyelectrolytic forces particularly that from the release of condensed counter ions from the RNA helix upon binding of charged ligands. The free energy of binding of berberine, palmatine and ethidium to t-RNA and the polyelectrolytic and the non-polyelectrolytic contribution to the same were calculated and presented in Table 4. Fig. 7B shows a graphical representation of the contribution of ΔG_t and ΔG_{pe} to the overall binding free

Table 4
Energetics of binding of berberine, palmatine and ethidium to t-RNA[a]

Compound	$K_i/10^5$ (M^{-1})	$-\Delta G^o_{obsd}$	$-\delta$ log K_i/δlog [Na^+]	$-\Delta G_t$ (kcal/mol)	$-\Delta G_{pe}$ (kcal/mol)
Berberine	1.15±0.20	6.89	0.24	5.91	0.98
Palmatine	1.05±0.30	6.84	0.34	5.45	1.39
Ethidium	1.38±0.30	7.00	0.14	6.43	0.57

[a]Binding constants (K_i) and standard free energy changes refer to solution conditions of CP buffer containing 0.5 mM Na_2HPO_4, pH 7.0 at 25 °C. The parameters are as defined in the text. The free energy change was deduced from the difference $(\Delta G_t) = \Delta G^o_{obsd} - \Delta G_{pe}$. The error in ΔG_{pe} is around 0.06 kcal/mol and the propagated error in ΔG_t is about 0.3 kcal/mol.

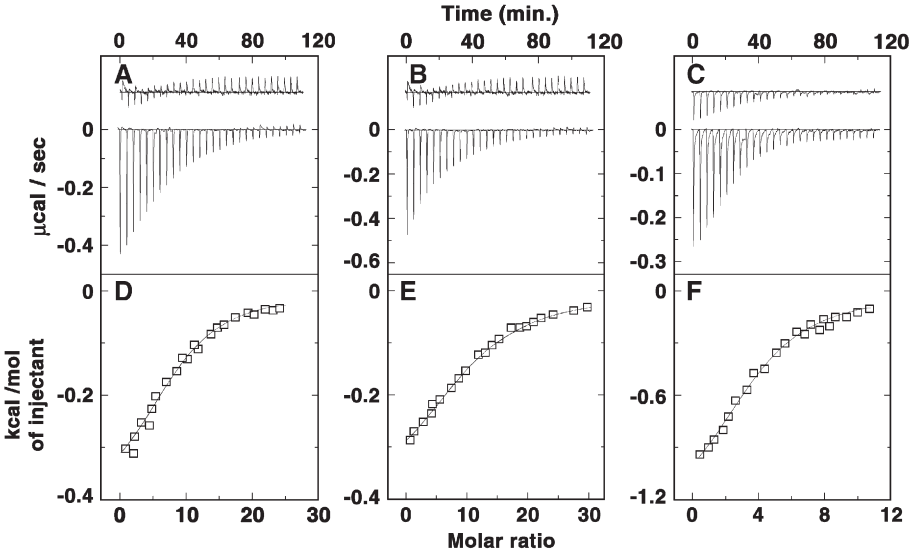

Fig. 8. ITC profile for the binding of berberine, (A and D) palmatine (B and E), and ethidium (C and F) to t-RNA at 25 °C in CP buffer of pH 7.0. The top panels (A, B and C) represent the raw data for sequential injection of t-RNA into the ligands (curves on the bottom) and t-RNA dilution control (curves offset for clarity). The bottom panels (D, E and F) show the integrated heat data after correction of the heat of dilution of RNA against the molar ratio of each drug to t-RNA. The data (open squares) were fitted to a one-site model and the solid lines represent the best-fit of the data.

energy of berberine, palmatine and ethidium. It can be seen from the table and the figure that in all the three cases there is remarkably large magnitude from the non-electrostatic forces to the binding free energy.

3.9. Viscosity

Intercalation of various ligands between the base pairs of natural and synthetic DNAs as well as synthetic RNA polynucleotides has been shown to result in increase in viscosity arising from increased lengthening and stiffening of the chain [9,55]. Although t-RNA is not a rod like molecule, we investigated whether the effect of binding of these molecules has any effect on the intrinsic viscosity. The results (not shown) revealed that the binding of all the three compounds had profound effect on the intrinsic viscosity of t-RNA although the net increase was larger and the change steeper in case with ethidium.

3.10. Isothermal titration calorimetry

Isothermal titration calorimetry (ITC) has become an important tool for direct and reliable measure of the thermodynamic parameters of interaction of small molecules to biopolymers [56]. Since ITC measures heat exchange, it provides a reliable tool independent of the spectroscopic changes that occur in the reaction. Initially, the ITC experiments performed with alkaloid injection to t-RNA in the calorimetric cell revealed complex thermograms with no constant heat evolved at any point. Further, the large heats of dilution of the drugs have resulted in huge errors in the estimation of the thermodynamic parameters from the procedure employed. Furthermore, the use of simpler models to fit the thermograms resulted in extremely larger chi-square values that were unacceptable. Since, the stoichiometry of the binding was independently estimated by Job plots we choose to perform the reverse titration, keeping a constant concentration of the ligand in the calorimeter cell and progressively injecting t-RNA from the syringe. The ITC profiles for the binding of berberine, palmatine and ethidium to t-RNA shown in Fig. 8A, B and C displayed that the binding was exothermic in each case resulting in negative peaks in the plots of power versus time. The upper panels in the figure indicate representatively the raw ITC curves resulting from the injections of t-RNA into the solutions of these compounds. Each of the heat burst curves in the figure corresponds to a single injection. These injection heats were corrected by subtracting the corresponding dilution heats derived from the injection of identical amounts of RNA into buffer alone. The resulting corrected heat plotted as a function of molar ratio is depicted in the lower panel. The data points reflect the experimental injection heats while the solid lines reflect the calculated fits of the data. The injection heat data in all the three cases were fitted to a single set of identical sites

Table 5
ITC derived thermodynamic profiles for the binding of berberine, palmatine and ethidium to yeast t-RNA at 25 °C[a]

Parameters	Berberine	Palmatine	Ethidium
K_b /10^5 (M^{-1})	1.29±0.27	1.26±0.29	1.32±0.32
N	0.11	0.09	0.25
ΔG^o (kcal/mol)	−6.97	−6.95	−6.98
ΔH^o (kcal/mol)	−3.88	−4.47	−5.44
ΔS^o (cal/mol/K)	10.37	8.33	5.17

[a]All the data in this table are derived from ITC experiments conducted in CP buffer, pH 7.0. K_b and ΔH^o values were determined from fits of the ITC profiles, with indicated errors reflecting standard deviations of the experimental data from the fitted curves. The values of ΔG^o were determined using the equation $\Delta G^o = -(RT \ln K_b)$. The values of ΔS^o were determined using equation $\Delta G^o = \Delta H^o - T\Delta S^o$.

model and the model employed was the one yielding a reasonable fitting of the experimental data. The thermodynamic parameters for the binding of berberine, palmatine and ethidium obtained at 25 °C are summarized in Table 5. In case of berberine (Fig. 7A and D), the ITC data yielded an association constant (K_b) of $(1.29\pm0.27)\times10^5$ M^{-1}, a ΔH^o of −3.88 kcal/mol, $\Delta S^o=10.37$ cal/mol/K and a binding site size (1/N) of about 9 nucleotides while the values for palmatine binding (Fig. 7B and E) were (K_b) of $(1.26\pm0.29)\times10^5$ M^{-1}, a ΔH^o of −4.47 kcal/mol, $\Delta S^o=8.33$ cal/mol/K and a binding site size of about 11 nucleotides. The ITC data of ethidium to t-RNA complexation (Fig. 7C and F) yielded a K_b of $(1.32\pm0.31)\times10^5$ M^{-1}, a $\Delta H^o=-5.44$ kcal/mol, a ΔS^o of 5.17 cal/mol/K and a binding site size of 4 nucleotides.

4. Discussion

t-RNAs are polyribonucleotides with about eighty nucleotide units arranged in the shape of a cloverleaf (Fig. 1). They exhibit a diversity of well characterized secondary and tertiary structural features. t-RNAs contain four stem region and three loop regions. In the three-dimensional structure, the acceptor T-stem forms a continuous RNA double helix while the D-stem and the anticodon stem are stacked upon each other to form another double helix [57]. Although only about forty bases are involved in Watson-Crick base pairing in t-RNA, large part of the structure contain stacked base pairs. The primary aim of this study was to understand the t-RNA binding features of two novel natural alkaloids, berberine and palmatine that are known to exhibit myriad biological properties [27–34] and have remarkable DNA binding activities [35–40]. Further, not much is known on the RNA binding of these alkaloids except that berberine and palmatine were shown to bind with remarkable affinity to poly(A)[22–25] and very weakly to the Watson-Crick base paired A-form of poly(rC).poly(rG) [9].

From the results presented here it is clear that both the alkaloids bind well to the complex structure of t-RNA, which is being compared directly with the binding of the classical DNA intercalator ethidium. Initially, we sought to characterize the temperature and pH dependent transitions in t-RNA that confirmed that the native cloverleaf structure of the t-RNA is retained under the conditions of our study. It may be noted that numerous studies have emphasized the role of Mg^{2+} in the stabilization of the structural elements of t-RNA and it is now generally agreed that the presence of divalent cations like Mg^{2+} was absolutely required for proper folding and nativeness of the t-RNA [[58–62] and references therein]. At the same time it is likely that some folded structure could persist in the absence of Mg^{2+}, but at high [Na^+] conditions. In our studies no Mg^{2+} was present and under this condition, the cloverleaf structure of t-RNA appears to be maintained. pH dependent studies indicate that t-RNA undergoes protonation induced acid denaturation that was reversible as seen from the total recovery of the CD pattern on raising the pH back to 7.0. Previous studies have suggested moderate conformational change and likely protonation of adenines and cytosines to occur in acidic conditions, but no specific conclusions were suggested except that the stability of the t-RNA was influenced in the protonated conditions [63,64]. The results of the circular dichroic studies performed at low salt conditions here, suggest protonation induced denaturation of t-RNA, but the initial structure is more or less regained on reversing the solution pH to neutral condition. t-RNA also undergoes heat denaturation and renaturation, but no indication of any fine structure was revealed from the circular dichroic spectra. Again, the optical melting curve also could not reveal any complexity in the t-RNA melting. However, we have observed that three melting transitions in the DSC thermogram, a major unfolding and two satellite meltings on either side of the major transition. Similar behaviour to that observed here has been reported by other investigators at higher [Na^+] concentrations in t-RNA and also using NMR in the thermal unfolding of t-RNA and has been interpreted as the initial melting of the acceptor and anticodon stems followed by the TψC stem [65–67]. It may be noted that compared to the DSC profile, the spectroscopic changes viz. the optical melting profile and the CD melting were less informative in that only hyperchromicity or ellipticity variations were apparent. The average melting transition in optical UV melting, however, corresponds to the major DSC transition (T_m around 50 °C). In our studies we have chosen to retain low salt [Na^+] concentration assuming that the binding of these charged alkaloids may be remarkably influenced by the presence of divalent cations. In our hands, the CD spectral results indicated that pH and temperature variation denatured the t-RNA structure but the transition was more or less reversible and the RNA folds back to the native cloverleaf structure on reversing the temperature and the pH. Similarly, the optical thermal melting studies and the DSC scans were reproducible on rescan of the cooled sample underscoring the reversibility of the conformation of the t-RNA under the condition of our investigation. Nevertheless, we observe that the ratio between the calorimetric enthalpy (ΔH_{cal}) and the van't Hoff enthalpy (ΔH_v) obtained for the thermal unfolding of t-RNA is not unity as should have been the case for truly cooperative reversible transitions, indicating that the melting of t-RNA may not be exhibiting a simple two state unfolding behaviour. Although a detailed molecular interpretation of this discrepancy is outside the scope of the present paper, it is relevant to point out that such discrepancies may also arise due to inaccuracies in the determination of t-RNA concentrations. It may be noted from the literature that widely different molar extinction coefficient values in the range 10^3–10^5 have been employed by different workers for the determination of the concentration of $t\text{-RNA}^{phe}$. In any case this discrepancy does not affect the interpretation of the results of our binding studies of the alkaloids and ethidium to the t-RNA structure as the binding studies have all been performed at one temperature viz. 25 °C.

The strong binding of the two alkaloids palmatine and berberine and ethidium to t-RNA was revealed prima facie from absorption spectral studies that indicated remarkable hypochromic and bathochromic effects with clear isosbestic points in each system. In many drug–nucleic acid systems, particularly in studies with DNA, such features observed have been more often thought in terms of intercalation between base pairs although the results have been conclusively interpreted in combination

with hydrodynamic data. Nevertheless, similar changes observed in all of the three drugs studied here indicated an intimate and strong association of the alkaloids and ethidium to t-RNA structure. We have observed a strong enhancement in the fluorescence of these molecules on interaction with t-RNA. The enhancement was comparable in case of both the alkaloids, but was significantly higher in case of ethidium. This further indicates that the bound molecules are similarly located in regions of higher polarity, apparently deep inside the base pairs. The analysis of the binding data both from spectrophotometric and fluorimetric studies revealed that the alkaloids bind t-RNA with slightly lower affinity compared to ethidium (Table 3). The number of binding sites obtained by these analysis was in good agreement with the stoichiometry estimated from the jobs plot. The alkaloids are found to occupy more nucleotide bases on t-RNA compared to ethidium the reason for which is not very clear. Such higher numbers for occluded sites have been observed for their binding to DNA also [36,39]. We have also observed that the viscosity of the t-RNA molecules increased more rapidly in the presence of ethidium and weakly in the presence of both the alkaloids, and this result in combination with competitive fluorescence quenching experiments (not shown) again suggested a stronger binding of ethidium molecules compared to the alkaloid molecules. Circular dichroic studies (not shown) of t-RNA complexation with berberine and palmatine revealed conformational change manifested by the decrease of the molar ellipticity of the 269 nm band of t-RNA. While no induced CD was seen in the complexation with the alkaloids, the appearance of large induced positive CD band in the 320 nm region, the hallmark of ethidium intercalation [68], was apparent with t-RNA. It is pertinent to observe that ethidium is a planar molecule while berberine and palmatine are buckled molecules that may preclude them from binding between base pairs as classical intercalators.

The analysis of the salt dependence of the binding free energy of the interaction revealed interesting features. The binding free energy has been observed to have remarkably large contribution from the non-electrostatic free energy. The non-electrostatic contribution to the overall free energy is similar in all the three cases indicating that the binding in each case is similarly stabilized to an equal extent by van der Walls stacking and hydrophobic interactions. It may be noted that there are no H-bonding centers in any of these compounds to contribute to the non-electrostatic free energy. The polyelectrolytic contribution to the free energy in each case is less than 1 kcal/mol and is significantly lower with ethidium.

The energetics of the interaction profiles of these molecules was revealed from the isothermal titration calorimetric studies. An interesting feature of the thermodynamic data (Table 5) is that despite differences in the structure and planarity of the molecules, there is little variation in apparent free energies. The binding of the alkaloids was exothermic and driven by a moderately favourable enthalpy decrease in combination with a moderately favourable entropy increase. It is likely that the alkaloid binding is associated by a variety of noncovalent molecular interactions like intercalation of the chromophore into the adjacent base pairs of t-RNA and van der Walls interaction that contribute to the negative enthalpy change. Further, it may be noted that the buckled structure of the alkaloids due to the partial saturation in the polycondensate ring system on binding/intercalation to t-RNA might lead to considerable distortion in the t-RNA helix and relaxation of the supercoiling that might in turn cause some disruption of ordered water structure. In the case with ethidium, the binding is driven by a large favourable enthalpy decrease. Previous reports of binding of some small molecules on t-RNA have indicated single binding events; for e.g. the interaction of Ru(II) complex with yeast t-RNA studied by isothermal titration calorimetry suggested the binding to be driven by a combination of enthalpy and entropy leading to intercalation of the metal ions to t-RNA while the intercalative binding of $[Ru(phen)2PMIP]^{2+}$ was driven by a moderately favourable enthalpy decrease in combination with a moderately favourable entropy increase [69]. On the other hand a complex binding phenomenon has been reported from isothermal titration calorimetric studies of aminoglycoside-rRNA recognition [70,71]. The binding affinity determined from ITC studies reveals a slightly higher value for ethidium to t-RNA compared to the alkaloids, a trend that has been revealed from spectroscopic studies as well. It is noteworthy that absolute values are in excellent agreement with the spectroscopic data. Further, the apparent stoichiometry (*N*) values estimated from ITC are in good agreement with the values obtained from Jobs plot. The reciprocal values of (1/N) viz. 9, 11 and 4 obtained from ITC for berberine, palmatine and ethidium were also are in reasonable agreement with the exclusion site values from spectroscopic data although the absolute magnitudes and direct correlation of them may be viewed with caution as suggested by Cooper and coworkers [72].

It is perhaps pertinent to observe that several earlier biophysical and NMR studies of t-RNA with ethidium have suggested intercalation mode [73–77]. Contrary to this the subsequent crystal structure data suggested no evidence for intercalation [78]; instead the ethidium has been suggested to be located stacked over the base pairs isolated from the solvent. The observed binding reported from spectroscopic studies was characterized by electrostatic, H-bonding interactions. But more recent ^{19}F and ^{1}H NMR spectroscopic studies [79] of t-RNAs labeled with fluorine with ethidium advanced the view of ethidium intercalation into the acceptor stem of $t\text{-}RNA^{val}$ with no sequence selectivity. Our studies also lend support to the intercalative binding of ethidium on t-RNA being driven by the initial electrostatic interaction between the negatively charged phosphate oxygen and the positively charged phenanthrinic ring. The binding data for berberine and palmatine to t-RNA were close and similar to that with ethidium indicating similar binding mechanisms, but since the alkaloids are buckled, they may not be inserted fully like ethidium and this would probably be the reason for their observed lower affinities.

It is important to note that in comparison to the binding affinities of these alkaloids to DNA reported earlier [22–27] the values obtained for t-RNA appear to be nearly an order lower. Nevertheless, it is very significant to observe that these natural

alkaloids show considerable affinity to complex t-RNA structure in the context of the suggestions from ongoing research that has proposed diverse pharmacological potencies for protoberberines. Therefore it is not unlikely that apart from the stronger DNA binding, the apparently close t-RNA binding affinity also may play significant role in the molecular action of these alkaloids. A complete elucidation of the molecular basis of various biological actions of protoberberines thus must await further investigations.

Acknowledgements

Md. Maidul Islam and Dr. Rangana Sinha were supported by the Junior Research Fellowship (JRF, NET) and Research Associateship respectively of the Council of Scientific Research (CSIR), Government of India. The authors are grateful to Prof. Siddhartha Roy, Director, Indian Institute of Chemical Biology, for creating the calorimetric facility at this institute and to Dr. M. Maiti, CSIR Emeritus Scientist, for the critical reading of the manuscript. The authors also thank all the colleagues of the Biophysical Chemistry Laboratory for their help and cooperation at every stage of this work.

References

[1] M. Maiti, G.S. Kumar, Molecular aspects on the interaction of protoberberine, benzophenanthridine and aristolochia group of alkaloids with nucleic acid structures and biological perspectives, Med. Res. Rev. (in press), doi:10.1002/med.20087.
[2] L.H. Hurley, Secondary DNA structures as molecular targets for cancer therapeutics, Biochem. Soc. Trans. 29 (2001) 692–696.
[3] P.B. Dervan, Molecular recognition of DNA by small molecules, Bioorg. Med. Chem. 9 (2001) 2215–2235.
[4] J.B. Chaires, Drug–DNA interactions, Curr. Opin. Struct. Biol. 8 (1998) 314–320.
[5] A.W. McConnaughie, J. Spychala, M. Zhao, D. Boykin, W.D. Wilson, Design and synthesis of RNA-specific groove-binding cations: implications for antiviral drug design, J. Med. Chem. 37 (1994) 1063–1069.
[6] Y. Tor, RNA and the small molecule world, Angew Chem. Int. Ed. 38 (1999) 1579–1582.
[7] T. Hermann, Strategies for the design of drugs targeting RNA and RNA–protein complexes, Angew Chem. Int. Ed. 39 (2002) 1890–1904.
[8] T. Hermann, Rational ligand design for RNA; the role of static structure and conformational flexibility in target design, Biochimie 84 (2002) 869–875.
[9] R. Sinha, Md.M. Islam, K. Bhadra, G.S. Kumar, A. Banerjee, M. Maiti, The binding of DNA intercalating and non-intercalating compounds to A-form and protonated form of poly(rC)·poly(rG): spectroscopic and viscometric study, Bioorg. Med. Chem. 14 (2006) 800–814.
[10] P.G. Higgs, RNA secondary structure: physical and computational aspects, Quat. Rev. Biophys. 33 (2000) 199–253.
[11] T.R. Sosnick, T. Pan, RNA folding: models and perspectives, Curr. Opin. Struct. Biol. 13 (2003) 309–316.
[12] T. Hermann, E. Westhof, RNA as a drug target: chemical, modeling, and evolutionary tools, Curr. Opin. Biotechnol. 9 (1998) 66–73.
[13] K. Xavier, P.S. Eder, T. Giordano, RNA as a drug target: methods for biophysical characterization and screening, Trends Biotechnol. 18 (2000) 349–356.
[14] J. Gallego, G. Varani, Targeting RNA with small molecule drugs: therapeutic promise and chemical challenges, Acc. Chem. Res. 34 (2001) 836–843.
[15] Q. Vicens, E. Westhof, Molecular recognition of aminoglycoside antibiotics by ribosomal RNA and resistance enzymes: an analysis of X-ray crystal structures, Biopolymer 70 (2003) 42–57.
[16] D.P. Arya, Aminoglycoside-nucleic acid interactions: the case of neomycin, Top. Curr. Chem. 253 (2005) 149–178.
[17] F.A. Tanious, J.M. Veal, H. Buczak, L.S. Ratmeyer, W.D. Wilson, DAPI (4′,6-diamidino-2-phenylindole) binds differently to DNA and RNA: minor-groove binding at AT sites and intercalation at AU sites, Biochemistry 31 (1992) 3103–3112.
[18] M. Zhao, L. Janda, J. Nguyen, L. Strekowski, W.D. Wilson, The interaction of substituted 2-phenylquinoline intercalates with poly(A).poly (U): classical and threading intercalation modes with RNA, Biopolymers 34 (1994) 61–73.
[19] M. Fernandez-Saiz, F. Werner, T.M. Davis, H.-J. Schneider, W.D. Wilson, Studies on the unique RNA duplex destabilization by an azoniacyclophane—NMR titrations with mono- and oligonucleotides of the RNA and DNA types, Eur. J. Org. Chem. 2002 (2002) 1077–1084.
[20] J.-J. Toulme, C. Helene, Anti messenger oligodeoxyribonucleotides: an alternative to antisense RNA for artificial regulation of gene expression—a review, Gene 72 (1988) 51–58.
[21] C. Helene, J.-J. Toulme, Specific regulation of gene expression by antisense, sense and antigene nucleic acids, Biochim. Biophys. Acta 1049 (1990) 99–125.
[22] R. Nandi, D. Debnath, M. Maiti, Interactions of berberine with poly(A) and tRNA, Biochim. Biophys. Acta 1049 (1990) 339–342.
[23] R.C. Yadav, G.S. Kumar, K. Bhadra, P. Giri, R. Sinha, S. Pal, M. Maiti, Berberine, a strong polyriboadenylic acid binding plant alkaloid: spectroscopic, viscometric, and thermodynamic study, Bioorg. Med. Chem. 13 (2005) 165–174.
[24] P. Giri, M. Hossain, G.S. Kumar, RNA specific molecules: cytotoxic plant alkaloid palmatine binds strongly to poly(A), Bioorg. Med. Chem. Lett. 16 (2006) 2364–2368.
[25] P. Giri, M. Hossain, G.S. Kumar, Molecular aspects on the specific interaction of cytotoxic plant alkaloid palmatine to poly(A), Int. J. Biol. Macromol. 39 (2006) 210–221.
[26] F. Xing, G. Song, J. Ren, J.B. Chaires, X. Qu, Molecular recognition of nucleic acids: coralyne binds strongly to poly(A), FEBS Lett. 579 (2005) 5035–5039.
[27] A.H. Amin, T.V. Subbaiah, K.M. Abbasi, Berberine sulfate: antimicrobial activity, bioassay, and mode of action, Can. J. Microbiol. 15 (1969) 1067–1076.
[28] W.A. Creasey, Biochemical effects of berberine, Biochem. Pharmacol. 28 (1979) 1081–1084.
[29] T. Schmeller, B. Latz-Bruning, M. Wink, Biochemical activities of berberine, palmatine and sanguinarine mediating chemical defence against microorganisms and herbivores, Phytochemistry 44 (1997) 257–266.
[30] C.L. Kuo, C.W. Chi, T.Y. Liu, Modulation of apoptosis by berberine through inhibition of cyclooxygenase-2 and Mc1-1 expression in oral cancer cells, In Vivo 1 (2005) 247–252.
[31] S. Nishida, S. Kikuichi, S. Yoshioka, M. Tsubaki, Y. Fujii, H. Matsuda, M. Kubo, K. Irimajiri, Induction of apoptosis in HL-60 cells treated with medicinal herbs, Am. J. Chin. Med. 4 (2003) 551–562.
[32] S. Letašiová, S. Jantová, L. Čipák, M. Múčková, Berberine-antiproliferative activity in vitro and induction of apoptosis/necrosis of the U937 and B16 cells, Cancer Lett. 239 (2006) 254–262.
[33] S. Letašiová, S. Jantová, M. Miko, R. Ovadekova, M. Horvathova, Effect of berberine on proliferation, biosynthesis of macromolecules, cell cycle and induction of intercalation with DNA, ds DNA damage and apoptosis in Ehrlich ascites carcinoma cells, J. Pharm. Pharmacol. 58 (2006) 263–270.
[34] J.-M. Hwang, H.-C. Kuo, T.-H. Tseng, J.-Y. Liu, C.-Y. Chu, Berberine induces apoptosis through a mitochondria/caspases pathway in human hepatoma cells, Arch. Toxicol. 80 (2006) 62–73.
[35] D. Debnath, G.S. Kumar, R. Nandi, M. Maiti, Interaction of berberine chloride with deoxyribonucleic acids: evidence for base and sequence specificity, Indian J. Biochem. Biophys. 26 (1989) 201–208.
[36] G.S. Kumar, D. Debnath, A. Sen, M. Maiti, Thermodynamics of the interaction of berberine with DNA, Biochem. Pharmacol. 46 (1993) 1665–1667.
[37] A. Saran, S. Srivastava, E. Coutinho, M. Maiti, ^{1}H NMR investigation of the interaction of berberine and sanguinarine with DNA, Indian J. Biochem. Biophys. 32 (1995) 74–77.
[38] D.S. Pilch, C. Yu, D. Makhey, E.J. LaVoie, A.R. Srinivasan, W.K. Olson, R.R. Sauers, K.J. Breslauer, N.E. Geacintov, L.F. Liu, Minor groove-

directed and intercalative ligand-DNA interactions in the poisoning of human DNA topoisomerase I by protoberberine analogs, Biochemistry 36 (1997) 12542–12553.
[39] K. Bhadra, G.S. Kumar, S. Das, Md.M. Islam, M. Maiti, Protonated structures of naturally occurring deoxyribonucleic acids and their interaction with berberine, Biorg. Med. Chem. 13 (2005) 4851–4863.
[40] K. Bhadra, M. Maiti, G.S. Kumar, Molecular recognition of nucleic acids by small molecules: AT base pair specific intercalative binding of cytotoxic alkaloid palmatine (Communicated).
[41] T. Antony, M. Atreyi, M.V.R. Rao, Interaction of methylene blue with transfer RNA— a spectroscopic study, Chem. Biol. Inter. 97 (1995) 199–214.
[42] G. Gomori, in: S.P. Colowick, N.O. Kaplan (Eds.), Preparation of Buffers for Use in Enzyme Studies, in Methods Enzymol, vol. 1, Academic Press, 1955, pp. 138–146.
[43] G.S. Kumar, M. Maiti, DNA polymorphism under the influence of low pH and low temperature, J. Biomol. Struct. Dyn. 12 (1994) 183–201.
[44] S. Das, G.S. Kumar, M. Maiti, Conversions of the left-handed form and the protonated form of DNA back to the bound right-handed form by sanguinarine and ethidium: a comparative study, Biophys. Chem. 76 (1999) 199–218.
[45] R. Nandi, S. Chakraborty, M. Maiti, Base- and sequence-dependent binding of aristololactam β-D-glucoside to deoxyribonucleic acid, Biochemistry 30 (1991) 3715–3720.
[46] C.R. Cantor, P.R. Schimmel, Biophysical Chemistry Part III, pp. 1135–1139, W.H. Freeman, New York.
[47] C.Y. Huang, in: S.P. Colowick, N.O. Kaplan (Eds.), Determination of binding stoichiometry by the continuous variation method: the job plot, in Methods Enzymol, vol. 87, Academic Press, 1982, pp. 509–525.
[48] J.D. McGhee, P.H. von Hippel, Theoretical aspects of DNA-protein interactions: co-operative and non-co-operative binding of large ligands to a one-dimensional homogeneous lattice, J. Mol. Biol. 86 (1974) 469–489.
[49] A. Ray, M. Maiti, A. Nandy, Scatplot: a computer program for determination of binding parameters of non-linear non-cooperative ligand–substrate interactions, Comput. Biol. Med. 26 (1996) 497–503.
[50] A. Ray, G.S Kumar, M. Maiti, Molecular aspects on the interaction of aristololactam-β-D-glucoside with H^L-form deoxyribonucleic acid structures, J. Biomol. Struct. Dyn. 21 (2003) 141–151.
[51] L.A. Marky, K.J. Breslauer, Calculating thermodynamic data for transitions of any molecularity from equilibrium melting curves, Biopolymers 26 (1987) 1601–1620.
[52] J.B. Chaires, S. Satyanarayana, D. Suh, I. Fokt, T. Przewloka, W. Priebe, Parsing the free energy of anthracycline antibiotic binding to DNA, Biochemistry 35 (1996) 2047–2053.
[53] J.B. Chaires, Dissecting the free energy of drug binding to DNA, Anti-Cancer Drug Des. 11 (1996) 569–580.
[54] J.D. Ballin, I.A. Shkel, M.T. Record Jr., Interactions of the KWK_6 cationic peptide with short nucleic acid oligomers: demonstration of large Columbic end effects on binding at 0.1–0.2 M salt, Nucleic Acids Res. 32 (2004) 3271–3281.
[55] D. Suh, J.B. Chaires, Criteria for the mode of binding of DNA binding agents, Bioorg. Med. Chem. 3 (1995) 723–728.
[56] R. O'Brien, I. Haq, Applications of biocalorimetry: binding, stability and enzyme kinetics, in: J.E. Ladbury, M. Doyle (Eds.), Biocalorimetry, John Wiley and Sons Ltd., 2004.
[57] A. Rich, U.L. RajBhandary, Transfer RNA: molecular structure, sequence and properties, Ann. Rev. Biochem. 45 (1976) 805–860.
[58] A. Stein, D.M. Crothers, Conformational changes of transfer RNA, The role of magnesium (II), Biochemistry 15 (1976) 160–168.
[59] M.W. Friederich, P.J. Hagerman, The angle between the anticodon and aminoacyl acceptor stems of yeast tRNA(Phe) is strongly modulated by magnesium ions, Biochemistry 36 (1977) 6090–6099.
[60] M. Vives, R. Tauler, R. Gargallo, Study of the influence of metal ions on $tRNA^{Phe}$ thermal unfolding equilibria by UV spectroscopy and multivariate curve resolution, J. Inorg. Biochem. 89 (2002) 115–122.
[61] E.J. Maglott, S.S. Deo, A. Przykorska, G.D. Glick, Conformational transitions of an unmodified tRNA: implications for RNA folding, Biochemistry 37 (1998) 16349–16359.
[62] V. Serebrov, R.J. Clarke, H.J. Gross, L. Kisselev, Mg^{2+}-induced tRNA folding, Biochemistry 40 (2001) 6688–6698.
[63] M. Bina-Stein, D.M. Crothers, Conformational changes of transfer ribonucleic acid. The pH phase diagram under acidic conditions, Biochemistry 13 (1974) 2771–2775.
[64] M. Steinmetz-Kayne, R. Benigno, N.R. Kallenbach, Proton nuclear magnetic resonance study of the effect of pH on tRNA structure, Biochemistry 16 (1977) 1064–2073.
[65] R. Römer, D. Riesner, G. Maass, W. Wintermeyer, R. Thiebe, H.G. Zachau, Cooperative helix-coil transitions in half molecules of phenylalanine specific tRNA from yeast, FEBS Lett. 5 (1969) 15–19.
[66] D. Riesner, G. Maass, R. Thiebe, P. Philippsen, H.G. Zachau, The conformational transitions in yeast $tRNA^{Phe}$ as studied with $tRNA^{Phe}$ fragments, Eur. J. Biochem. 36 (1973) 76–88.
[67] G.T. Robillard, C.E. Tarr, F. Vosman, B.R. Reid, A nuclear magnetic resonance study of secondary and tertiary structure in yeast $tRNA^{phe}$, Biochemistry 16 (1977) 5261–5273.
[68] K.S. Dahl, A. Pardi, I. Tinoco Jr., Structural effects on the circular dichroism of ethidium ion–nucleic acid complexes, Biochemistry 21 (1982) 2730–2737.
[69] H. Xu, Y. Liang, P. Zhang, F. Du, B.-R. Zhou, J. Wu, J.-H. Liu, Z.-G. Liu, L.N. Ji, Biophysical studies of a ruthenium (II) polypyridyl complex binding to DNA and RNA prove that nucleic acid structure has significant effect on binding behaviors, J. Biol. Inorg. Chem. 10 (2005) 529–538.
[70] M. Kaul, D.S. Pilch, Thermodynamics of aminoglycoside-rRNA recognition: the binding of neomycin-class aminoglycosides to the A site of 16S rRNA, Biochemistry 41 (2002) 7695–7706.
[71] D.S. Pilch, M. Kaul, C.M. Barbieri, J.E. Kerrigan, Thermodynamics of aminoglycoside-rRNA recognition, Biopolymers 70 (2003) 58–79.
[72] K.M. Guthrie, A.D.C. Parenty, L.V. Smith, L. Cronin, A. Cooper, Microcalorimetry of interaction of dihydro-imidazo-phenanthridinium (DIP)-based compounds with duplex DNA, Biophys. Chem. (2006) (on line).
[73] R. Bittman, Studies of the binding of ethidium bromide to transfer ribonucleic acid: absorption, fluorescence, ultracentrifugation and kinetic investigations, J. Mol. Biol. 46 (1969) 251–268.
[74] T.T. Sakai, R. Torget, I. Josephine, C.E. Freda, S.S. Cohen, The binding of polyamines and of ethidium bromide to tRNA, Nucleic Acids Res. 2 (1975) 1005–1022.
[75] T. Tao, J.H. Nelson, C.R. Cantor, Conformational studies on transfer ribonucleic acid. Fluorescence lifetime and nanosecond depolarization measurements on bound ethidium bromide, Biochemistry 9 (1970) 3514–3524.
[76] C.R. Jones, D.R. Kearns, Identification of a unique ethidium bromide binding site on yeast $tRNA^{Phe}$ by high resolution (300 MHz) nuclear magnetic resonance, Biochemistry 14 (1975) 2660–2665.
[77] C.R. Jones, P.H. Bolton, D.R. Kearns, Ethidium bromide binding to transfer RNA: transfer RNA as a model system for studying drug–RNA interactions, Biochemistry 17 (1978) 601–607.
[78] M. Liebman, J. Rubin, M. Sundaralingam, Nonintercalative binding of ethidium bromide to nucleic acids: crystal structure of an ethidium-tRNA molecular complex, Proc. Natl. Acad. Sci. U. S. A. 74 (1977) 4821–4825.
[79] W.-C. Chu, J.C.-H. Liu, J. Horowitz, Localization of the major ethidium bromide binding site on tRNA, Nucleic Acids Res. 25 (1997) 3944–3949.